BIOSCIENCES BIOTECHNOLOGY RESEARCH ASIA, September 2024. Vol. **21**(3), p. 1063-1076

In Silico Evaluation of Marine Phytochemicals as Potential Inhibitors of Inhibitor-Kappa B Protein Kinase (IκK) for Alzheimer's Disease Therapeutics

Deepak Sheokand, Annu Grewal, Vivek Kumar, Raveena Chauhan, Vandana Saini and Ajit Kumar*

Toxicology and Computational Biology Group, Centre for Bioinformatics
Maharshi Dayanand University, Rohtak, Haryana, India.

http://dx.doi.org/10.13005/bbra/3286

(Received: 12 December 2023; accepted: 22 July 2024)

Alzheimer's disease (AD) is a polygenic, progressive neurodegenerative condition that leads to cognitive and behavioural impairment. The drugs available for AD have been found vital for symptomatic cognitive treatment, but cannot treat or slow down the disease's progression, besides having severe side effects. Plants have been extensively used in traditional medicine, and marine phytochemicals have also been proven as a legitimate solution for several ailments. This study was carried out to screen marine phytochemicals for AD therapy and neuroinflammation by focusing on inhibiting the neuroinflammatory pathway involved in AD progression and nervous system degeneration using I?K as the therapeutic target protein. Virtual screening of 2583 marine phytochemicals retrieved from the Comprehensive Marine Natural Products Database (CMNPD) was performed for Lipinski's rule, ADME/T profiling, Blood-brain permeability and molecular docking studies using I?K as the target receptor and Curcumin as the standard inhibitor of I?K. Seven marine phytochemicals (CMNPD IDs: CMNPD25050, CMNPD793, CMNPD18964, CMNPD14904, CMNPD31514, CMNPD24296) showed better binding affinity when docked against I?K as compared to the standard compound Curcumin and are the potential lead molecules to be further evaluated for AD therapy. Molecular dynamics simulations were also performed to investigate the binding interactions and stability of the top-hit marine phytochemical CMNPD25050 (8,11-dihydro-1-methoxy laurokamuren-12-ol) with the I?K target protein.

Keywords: Marine natural products; Molecular modelling; Molecular docking; Nuclear factor-kappa B (NF- κB); Virtual Screening.

Alzheimer's disease (AD) is the most common neurodegenerative ailment affecting about 24 million people worldwide, and it accounts for 50-70% of all cases of dementia[1]. The accumulation of amyloid-beta plaques (extracellular) and neurofibrillary tangles (intracellular) are considered to be the two pathological hallmarks of AD[2]. Many unequivocal hypotheses have been proposed regarding AD pathologies, based on amyloid protein accumulation, cholinergic pathway, and oxidative stress[3-6]. Neuroinflammation plays a crucial role in the pathogenesis of Alzheimer's disease. The presence of amyloid-beta and neurofibrillary tangles triggers an inflammatory response in the brain, characterized by the activation of glial cells (microglia and astrocytes) and the release of inflammatory mediators like cytokines, chemokines, and reactive oxygen

*Corresponding author E-mail: akumar.cbt.mdu@gmail.com

species. This chronic neuroinflammatory state exacerbates neuronal damage and contributes to the progression of the disease.

The nuclear factor-kappa B (NF-êB) has a pivotal role in the pathophysiology of Alzheimer's disease (Figure 1). In the cytoplasm, NF-êB remains masked for nuclear translocation through its association with the inhibitor-kappa B protein (IêB). Neuronal stimuli like – Tumor necrosis factor receptors (TNFRs), lipopolysaccharides (LPS), cytokines, etc, trigger the activation of IêB kinase (IêK), leading to IêB phosphorylation and degradation, and unmasked NF-êB translocates to the nucleus. Within the nucleus, NF-êB interacts with the promoter regions of key genes, such as BACE1 and APOE, involved in neurodegeneration and Alzheimer's disease progression (Figure 1). Thus NF-êB play the central role in in molecular events that drive Alzheimer's disease pathology, linking neuroinflammation, Aâ production, and neurodegeneration[7-8]. The expression of â-secretase1 (BACE1) is also regulated by the NF-êB signalling pathway, which increases Aâ production and accumulation[9]. The NF-êB pathway can be regulated in AD patients by inhibiting the factors responsible for its elevated level. Inhibition of IêK can break the thread of NF-êB-related pathophysiologies. The IêKs are also reported to be essential to various disease conditions such as asthma and rheumatoid arthritis[10], thus imperatively suggesting it to be considered as a possible therapeutic target for AD therapy[11].

Phytochemicals, including marine phytochemicals, have been demonstrated to have neuroprotective properties. Marine algae are a rich source of antioxidants like carotenoids, phenolics, sulfated polysaccharides, and vitamins that have exhibited neuroprotective properties in neuronal cell cultures and animal models[12]. The extracts from green algae (*Codium tomentosum*) have been shown to have neuronal cell protection from amyloid beta-induced toxicity through antioxidant effects and acetylcholinesterase inhibition[13]. Additionally, the phlorotannin compound EM2 isolated from the brown alga (*Ecklonia maxima*) was reported to reduce apoptosis and mitochondrial dysfunction in cellular Parkinson's disease models[14]. *In-vivo*, evidence also supports the neuroprotective effects of marine products. Supplementation with the lichen-derived ramalin improved cognitive function in an Alzheimer's mouse model by attenuating neuroinflammation and neuronal cell death[15]. These findings highlight the neuroprotective potential of certain marine natural products and warrant further research into their bioavailability, efficacy, and safety in human clinical trials. Marine compounds may provide promising new therapeutics for age-related neurodegenerative diseases.

So, the present study was undertaken to screen the marine phytochemicals, using *in-silico* tools to design and development of AD therapeutics. The virtual screening involved Druggability profiling (Lipinski's rule), ADME/T profiling, Blood-brain permeability and molecular docking studies, and Molecular dynamics simulations using IêK as the target receptor.

MATERIALS AND METHODS

Retrieval and pharmacokinetics screening of marine phytochemicals

Marine phytochemicals were retrieved from the Comprehensive Marine Natural Products Database (CMNPD) in plant taxa, and 2583 compounds were obtained on 26 May 2022[16] (Supple1_CMNPD). CMNPD is a manually curated open-access knowledge base dedicated to marine natural products research, currently containing 31561 compounds with unique chemical structures.

The library of marine phytochemicals was filtered to select molecules with drug-like properties and oral bioavailability. Key criteria that impact oral absorption and permeability were calculated, including hydrogen bond donors/acceptors, molecular weight, and partition coefficient (logP). Compounds were screened using the Sanjeevini web server[17] to identify those violating no more than one of Lipinski's guidelines. This widely utilized principle states that oral bioavailable medications tend to comply with cutoffs of <5 hydrogen donors, <10 hydrogen acceptors, molecular weight under 500 daltons, and logP not >5. ADMET (absorption, distribution, metabolism, excretion, and toxicity) properties, HIA (Human intestinal absorption), blood-brain barrier permeability, H-HT (Human hepatotoxicity), Ames's mutagenesis, DILI (Drug-induced liver injury), Herg inhibition, ROA (Rat Oral Acute Toxicity) and Respiratory toxicity of the

phytochemicals were analyzed using ADMETlab 2.0 [18] webserver. Compounds exhibiting favourable outcomes were selected for further investigations.

Retrieval and energy minimization of 3D structures of selected marine phytochemicals

The 3D structures of selected compounds, after pharmacokinetic screening, were retrieved from PubChem Database [19] in structure data file (.sdf) format. These ligands were exported in pdb format, using PyMOL[20]. The 3D structures of the ligand molecules were subjected to energy minimization, using the AMBERff14SB force field in UCSF Chimera[21], prior to docking. Minimization was performed using the steepest descent algorithm for 100 steps followed by conjugate gradient for 10 steps with a step size of 0.02 Å. This energy minimization relieved strain and brought the ligands to a lower energy conformation. *Curcumin* was selected as a standard compound as it serves as an IêK inhibitor[2-3].

Homology modelling and validation of target protein

The 3D structure of IêK protein, available at RCSB Protein Data Bank (PDB)[22] with PDB ID 4KIK, was observed to have several missing residues. Hence, homology modelling of IêK protein was done, using the SWISS-MODEL web server (https://swissmodel.expasy.org/) in user template mode, to obtain the complete 3D structure. The protein sequence of the IêK protein was retrieved from the Uniprot database (https://www.uniprot.org/) for homology modelling. The modelled 3D structure of IêK protein was validated using the ERRAT[23] and PROCHECK[24] of SAVESv6.0, ProSA-web[25] and MolProbity online servers. The validated target protein (IêK) was subjected to energy minimization using the AMBERff14SB force field in UCSF Chimera[21].

Molecular docking

The molecular docking studies were carried out to evaluate the inhibitory potentials of selected marine phytochemicals. These ligands were docked against IêK protein, using Autodock suite v4.2.6[26-27]. Kollman and Gasteiger charges were assigned to the receptor protein followed by the conversion of PDB structure files of IêK protein and selected marine phytochemicals into pdbqt format using autodock tools (ADT). The grid box parameters for the binding pocket were saved as grid parameter files (GPF) for protein receptors, and necessary map files were generated after the autogrid run. Based on the predicted binding site by blind docking, the grid box was set to 68Å x 54Å x 64Å centred at 55.851, 28.783, and -59.265 (X, Y, and Z-axis). Autogrid was executed to generate the necessary grid map files based on the grid box parameters. In Autodock, the Lamarckian genetic algorithm was applied as the conformational search method to execute molecular docking. One hundred independent docking runs were carried out for each ligand-IêK complex using a translation step size of 0.2 Å. The genetic algorithm parameters were set to a population size of 150, mutation rate of 0.02, crossover rate of 0.8, and cluster tolerance of 0.5 Å. Autodock was then run to perform automated docking simulations and calculate dock scores for each ligand. Finally, the interactions between the top dock-scoring phytochemical- IêK complexes were visualized using LIGPLOT+[28] to analyse the molecular interactions within the binding sites.

Molecular dynamic simulations

The top docked complex of marine phytochemical 8,11-dihydro-1-methoxy laurokamuren-12-ol with IêK protein was selected for further molecular dynamic simulation (MDS) study using GROMACS v2020.1[29-30]. The topology files for selected marine phytochemical and receptor complexes are generated using the Charmm 36m force field [31]. Then the selected simulation system was prepared by solvating the complex in a cuboid box with TIP3P water molecules, whereas to neutralize the system, sodium and chloride ions were added. After that, the geometric strain of the selected system was removed by energy minimization using the steepest descent algorithm. The simulation system, after undergoing energy minimization, was subjected to equilibration under constant temperature (310K) and pressure (1 bar) conditions for a duration of 1 nanosecond (ns) using the Nose-Hoover thermostat and Parrinello-Rahman barostat respectively, during the equilibration process. The system was studied for a period of 10 ns under constant temperature and pressure conditions, during the molecular dynamics simulation by employing periodic boundary conditions (PBC). Trajectory data was recorded at intervals of 1 picosecond (ps). Throughout the entire simulation, ligand-protein interaction was monitored to assess stability. To validate the binding stability of the selected

marine phytochemical with the studied Alzheimer's disease target receptor, several analyses were performed. These included calculations of the Root Mean Square Deviation (RMSD), root-mean-square fluctuation (RMSF), Coulombic and Lennard-Jones (LJ) interaction energies, Radius of gyration (Rg), and Solvent Accessible Surface Area (SASA) for each frame over the 10 ns simulation run.

RESULTS

Retrieval and pharmacokinetics screening of marine phytochemicals

A total of 2583 compounds were retrieved from CMNPD (Supple1_CMNPD) of which only 1485 phytochemicals were selected for drug-like properties based on lipinski's rule of five (Supple1_LIPINSKI).

Pharmacokinetic profiling of the selected 1485 phytochemicals was conducted and a total of 122 phytochemicals (Supple1_ADMET) were obtained as hits with acceptable Absorption, distribution, metabolism, excretion and toxicity profiles using ADMETlab 2.0[18] and were selected for further molecular docking studies.

Homology modelling and model evaluation

The 3D-structure of the selected target protein (IêK protein) was obtained by comparative modelling using Uniprot id_O14920 (human IêK protein) sequence and PDB ID: 4KIK as a template by SWISS MODEL server (https://swissmodel.expasy.org/) in user template mode (Figure 2). The Ramachandran plot evaluation showed 94.3 % and 5.6% residues in favoured and additionally favoured regions, respectively revealing the model above good quality with an acceptable model score (Figure 3). The protein model of human IêK protein structure validation result using errat and procheck showed an Overall Quality Factor and Z-score of 93.92 (Figure 4) and -11.49, respectively. Additional MolProbity validation was performed on the completed IêK structure model, with results summarized in Table 1. Key quality metrics such as the clash score in the 99th percentile, good rotamers (2.54% outliers), and MolProbity score in the 80th percentile confirm the high stereochemical quality. The Ramachandran plot for the structure

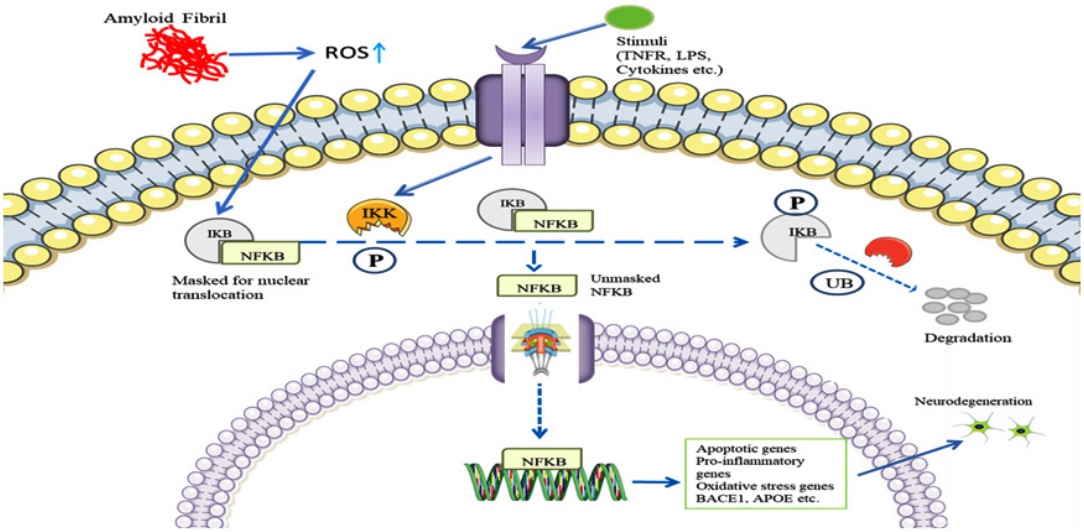

Fig. 1. Process of activation of NF-κB pathway and activation of genes involved in neurodegeneration, highlighting the central role of NF-κB in molecular events that drive Alzheimer's disease pathology, linking neuroinflammation, Aβ production, and neurodegeneration. In the cytoplasm, NF-κB remains masked for nuclear translocation through its association with the inhibitor-kappa B protein (IêB). The neuronal stimulation triggers the activation of IκB kinase (IκK), leading to IκB phosphorylation and degradation. The unmasked NF-κB translocates to the nucleus where it interacts with the promoter regions of key genes, such as BACE1 and APOE, involved in neurodegeneration and Alzheimer's disease progression

still shows some non-ideality, with 9.04% outliers and 81.92% favoured residues. However, overall results across multiple validation approaches verify this IêK homology model is of suitable accuracy for reliable molecular docking studies and further analyses.

Molecular docking studies

The selected 122 phytochemicals, with drug likeness and a good ADME/T profile, were subjected to molecular docking against a human IêK target protein, using Autodock suite v4.2.6, and their binding energies were noted (Supple1_ RESULT). The docking conformations of ligands (selected phytochemicals) showing binding energies lower than the selected standard (Curcumin) with a binding energy of -8.63kCal/mol, were selected for further study (Table 1). The seven hit phytochemicals (CMNPD IDs: CMNPD25050, CMNPD793, CMNPD18964, CMNPD14904, CMNPD31514, CMNPD24296) exhibited higher binding affinity towards the nuclear factor kappa-B kinase subunit beta as compared to Curcumin (Table 2). The docked complexes were visualized in PyMOL (20) and the ligand-protein interactions for the selected hits were analyzed by LIGPLOT+ to identify key interacting residues (Figure 6-7) (Table 3). The dock site analyses revealed all the studied ligands occupied a similar binding pocket as the standard (Curcumin), indicating their inhibitory actions (Figure 6-7). These selected phytochemicals were observed to be produced by two plant genera - *Ceriops* (Mangroves) and *Laurencia* (Red algae) (Table 2).

Molecular dynamics simulations

The root-mean-square deviation (RMSD) profile of the 8,11-dihydro-1-methoxy laurokamuren-12-ol and IêK complex was analyzed to evaluate the structural stability during the 10ns simulation. During the initial phase of approximately 1 ns, a rapid increase in RMSD is observed, indicating a major conformational rearrangement as the system departs from the starting structure. Subsequently, the RMSD fluctuates around a value within an acceptable range (0.3nm), suggesting that the complex attains a stable conformation after the initial equilibration period till the 10ns simulation (Figure 7a). The root-mean-square fluctuation (RMSF) analysis revealed significant fluctuations in the mobility and flexibility of different regions within the protein structure. The RMSF values ranged from a minimum of 0.0537 (residue 3273) to a maximum of 0.6605 (residue 10628), indicating the presence of both rigid and highly flexible regions. Several distinct peaks like residue 10621 with RMSF of 0.6134nm were observed in the RMSF profile, suggesting the presence of flexible loops, hinges, or exposed domains (Figure 7a). In contrast, several regions exhibited relatively low RMSF values, indicating more rigid and stable portions of the protein structure (Figure 7b). The total

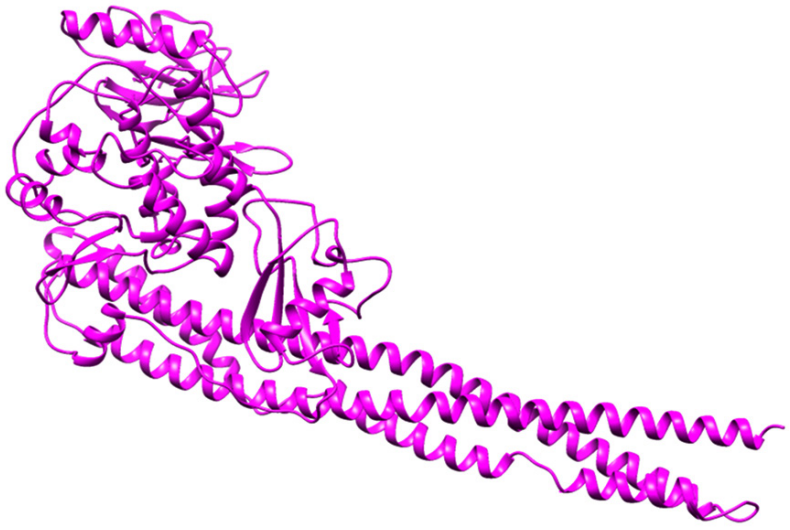

Fig. 2. The 3D structure of human IκK protein modelled structure

radiation of gyration (rGyr) values reported in the data range from a minimum of approximately 5.78 nm to a maximum of around 5.81 nm, with an average value of approximately 5.80 nm over the 10 nanosecond simulation trajectories (Figure 7c). The relatively small variations observed in the rGyr, with a range of approximately 0.03 nm, suggesting that the overall size and compactness of the system remained relatively stable throughout the simulation (Figure 7c). The total interaction energy between the ligand and protein was analyzed from the 10ns molecular dynamics trajectory. The Coulombic interaction energy was found to be -38.6352 kJ/mol, indicating favourable electrostatic interactions between the ligand and protein. However, the Lennard-Jones interaction energy was 289.744 kJ/mol, suggesting significant steric clashes or unfavourable van der Waals interactions. The total interaction energy exhibited fluctuations throughout the simulation, as evident from the energy profile (Figure 7e). The number of hydrogen bonds fluctuated significantly over 10ns times, ranging from 0 to 3 hydrogen bonds at different points during the simulation (Figure 7d). There were periods where no hydrogen bonds were present, as well as instances where multiple hydrogen bonds (up to 3) were formed simultaneously between the 8,11-dihydro-1-methoxy laurokamuren-12-ol and NF-êB protein. This variability in hydrogen bonding suggests a highly flexible binding mode, with the hydrogen bond interactions continually forming, breaking, and reforming throughout the 10ns simulation. The solvent-accessible surface area (SASA) of the

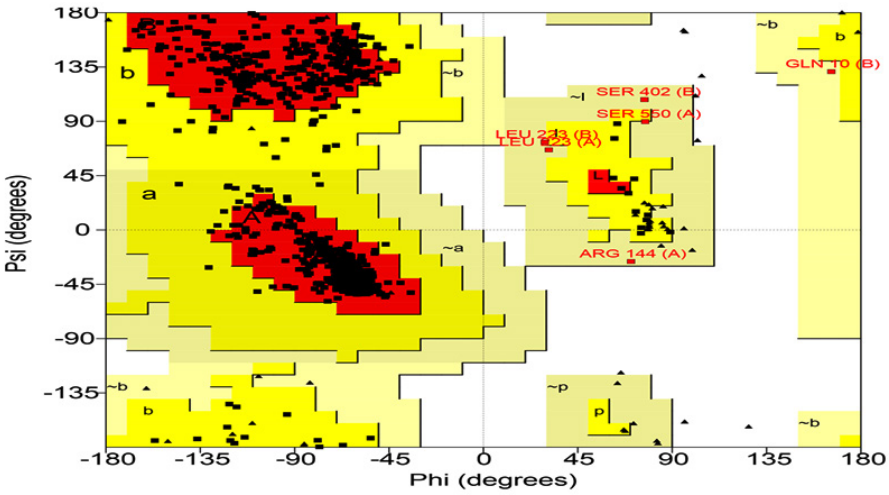

Fig. 3. The Ramachandran plot of modelled structure of IκK protein

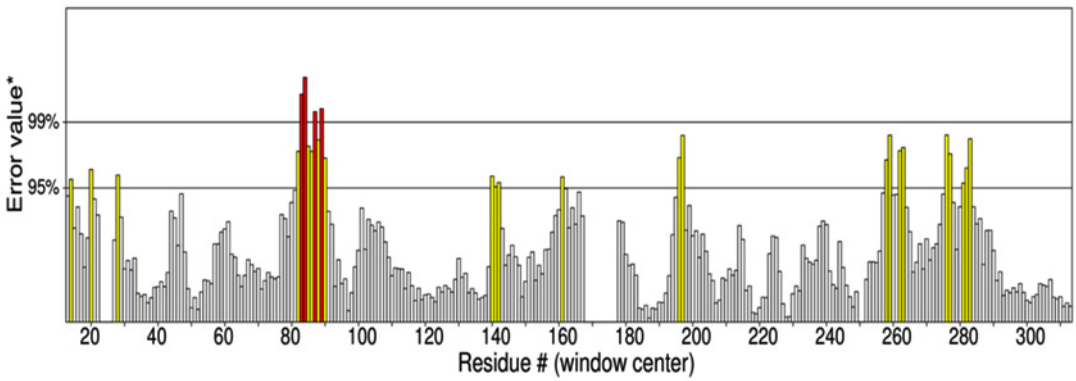

Fig. 4. The errat result of modelled structure of IκK protein

simulated system over the 10 ns time scale exhibits significant fluctuations, ranging from a minimum of approximately 6.45 nm to a maximum of around 7.73 nm (Figure 7f). These fluctuations indicate that the simulated system undergoes various conformational states during the simulation.

DISCUSSION

This in-silico study presents IêB kinase (IêK) as a therapeutic target for preventing the progression of AD using marine phytochemicals. A set of 2583 compounds, retrieved from CMNPD, were subjected to primary evaluation of druggability and having an acceptable ADME/T profile. Lipinski's rule of five parameters correlates with oral bioavailability[32](Supple1_LIPINSKI). ADMETlab 2.0 web server was used for ADME/T profiling. The algorithms in ADMETlab use machine learning on large experimental bioactivity datasets to predict property values[18]. The HIA model utilizes a robust random forest classifier trained on over 8000 compounds with human jejunal permeability data[33]. Blood-brain barrier permeability screening was done to select neuroactive candidates[34]. Hepatotoxicity, mutagenicity, cardiotoxicity, and other toxicity risks were minimized by filtering the compounds with low predicted liability [35-39]. An optimal probability cutoff of 0 to 0.7 was applied to select compounds with high gastrointestinal absorption, and neuroactive properties and minimize toxicity

Table 1. Summary of MolProbity validation metrics for the homology model of the human IκK protein

Validation metric	Result	Goal
Clashscore	1.54 (99th percentile)	Lower is better
Poor rotamers	2.54%	<0.3%
Ramachandran outliers	9.04%	<0.05%
Ramachandran favoured	81.92%	>98%
Molprobity score	1.918 (80th percentile)	Lower is better
Câ deviations	1.55%	0%
Bad bonds	0 / 27170 (0%)	0%
Bad angles	28 / 37080 (0.76%)	<0.1%
Cis prolines	0 / 32 (0%)	d"1 per chain
Cis non-prolines	2 / 3223 (0.62%)	<0.05%
Twisted peptides	28 / 3557 (7.89%)	0%
Cablam outliers	17 (4.8%)	<1.0%
CA Geometry outliers	9 (2.56%)	<0.5%
Chiral volume outliers	0 / 405	-

Table 2. The phytochemicals of CMNPD having binding energies lower than the standard (Curcumin), when docked against IκK protein

S. No.	CMNPD ID	Binding energy (kcal/mol)	Plant name	Compound Name
1.	CID969516	-8.63	*Curcuma longa*	Curcumin
2.	CMNPD25050	-11.35	*Laurencia obtusa*	8,11-dihydro-1-methoxy laurokamuren-12-ol
3.	CMNPD793	-10.41	*Laurencia pinnata*	Pinnasterol
4.	CMNPD775	-10.14	*Laurencia irieii*	Neoireone
5.	CMNPD18964	-9.41	*Laurencia saitoi*	No Data
6.	CMNPD14904	-9.28	*Laurencia tristicha*	10-hydroxyepiaplysin
7.	CMNPD31514	-8.95	*Ceriops decandra*	Decandrol D
8.	CMNPD24296	-8.69	*Ceriops decandra*	Decandrin B

[18], This multi-parameter ADMET filtration resulted in 122 out of evaluated marine phytochemicals and were selected for further molecular docking studies (Supple1_ADMET).

The target protein (human IêK enzyme) structure at Protein Databank (PDB), selected for our study, had missing residues (PDB ID: 4KIK) and hence was subjected to homology modelling to generate the complete 3D-structure, using SWISS-MODEL with the 4KIK crystal structure as a template (Figure 2). The generated 3D model of the human IêK enzyme was evaluated using multiple model validation assessment methods that confirmed model reliability for its subsequent use in molecular docking studies. The Ramachandran plot evaluation demonstrated excellent stereochemical quality, with 94.3% of residues in the most favoured regions and 5.7% in allowed regions [24] (Figure 3). No residue was detected in a disallowed region of the Ramachandran plot. The ERRAT evaluation of non-bonded interactions of the modelled structure of human IêK revealed an overall quality factor of 93.92% (Figure 4), exceeding the acceptable value of ~91%, for templates with 2.5-3.0Å resolution[23], thus confirming minimal structural error in our generated model of human IêK protein. The ProSA analysis revealed a Z-score of -11.49 that falls within the range characteristic of native proteins and reflected proper residues' packing of our modelled structure of human IêK [25,40]. MolProbity evaluation (Table 1) of the IêK homology model showed favourable metrics across several validation criteria. The Clashscore was 1.54, ranking in the 99th percentile relative to other structures and indicating excellent packing and absence of serious steric clashes. Only 2.54% of residues were flagged as poor rotamers. In terms of backbone geometry, 9.04% of residues were Ramachandran outliers, below the recommended <0.05%. 81.92% of residues were in favoured regions, slightly lower than the target >98%. The MolProbity score of 1.918 ranked in the 80th percentile. There were minimal deviations in bond lengths and angles, with 0 bad bonds and only 0.76% bad angles.

Table 3. Ligand-protein interactions for the selected hits (phytochemicals) of CMNPD having binding energies lower than the standard (Curcumin), when docked against IκK protein

S. No.	CMNPD ID	H-Bond	H-bond interaction	Interacting Residues
1.	*Curcumin*	5	Cys99-3.01 , Asp166-3.05, 2.46Lys44-3.17Thr23-2.90,3.18	Leu21, Gly22, Val29, Glu61, Met65, Leu94, Met96, Tyr98, Val152, Ile165
2.	CMNPD25050	2	Cys99-3.23Asp166-3.00	Leu21, Gly22, Thr23, Gly24, Phe26, Gly27, Val29, Ala42, Lys44, Val97, Tyr98, Gly102, Asp103, Val152, Ile165
3.	CMNPD793	4	Cys99-3.03,2.91Glu97-3.14,3.02	Leu21, Gly22, Thr23, Val29, Ala42, Val74, Met96, Tyr98, Gly102, Glu149, Val152, Ile165
4.	CMNPD775	5	Cys99-3.00,2.87Glu97-3.07 Thr23-2.97,3.09	Leu21, Gly22,Val29, Ala42, Lys44, Val74, Met96, Tyr98, Gly102, Glu149, Val152, Ile165
5.	CMNPD18964	4	Thr23-2.74,2.82Glu97-3.14 Cys99-3.19	Leu21, Gly22, Gly24, Phe26, Val29, Ala42, Tyr98, Gly102, Asp103, Glu149, Val152, Ile165
6.	CMNPD14904	5	Asp145-2.71,2.63, Lys147-2.86,Asn150-2. Asp166-2.83	Leu21, Gly22, Thr23, Gly24, Gly27, Val97, Tyr98,Cys99, Gly102, Asp103, Glu149, Val152, Ile165
7.	CMNPD31514	2	Glu97-3.15, Asp166-3.06	Gly22, Thr23, Gly24, Ala42, Lys44, Val74, Met96, Cys99, Gly102, Val152, Ile165
8.	CMNPD24296	2	Glu97-2.88, Cys99-3.24	Leu21, Gly22, Thr23, Val29, Ala42, Val74, Met96, Tyr98, Glu149, Asn150. Val152, Ile165

The percentage of twisted peptides at 7.89% was higher than ideal. The Cablam analysis identified 4.8% outliers in residue conformations and 2.56% outliers in CA geometry, both within acceptable ranges. There were no chiral volume outliers. Overall, the MolProbity validation indicates the IêK homology model exhibits excellent local packing and stereochemistry. The twisted peptides and marginally lower Ramachandran statistics are potential areas for improvement but are unlikely to significantly impact the suitability of the model for molecular docking studies. Comprehensively the model validation tools verified our homology model of human IêK protein as sufficiently accurate for its use in molecular docking studies.

Molecular docking was used in the present study to analyze the inhibitory effects of selected phytochemicals with Curcumin as a standard inhibitor of human IêK protein. Previous cellular and animal model studies have demonstrated the curcumin's ability to cross the blood-brain barrier[41-42] and exert anti-inflammatory effects in the CNS and research suggests these neuroprotective effects are mediated in part through inhibition of IêK protein and downstream NF-kB signaling [2-3]. AutoDock used for our molecular docking studies,

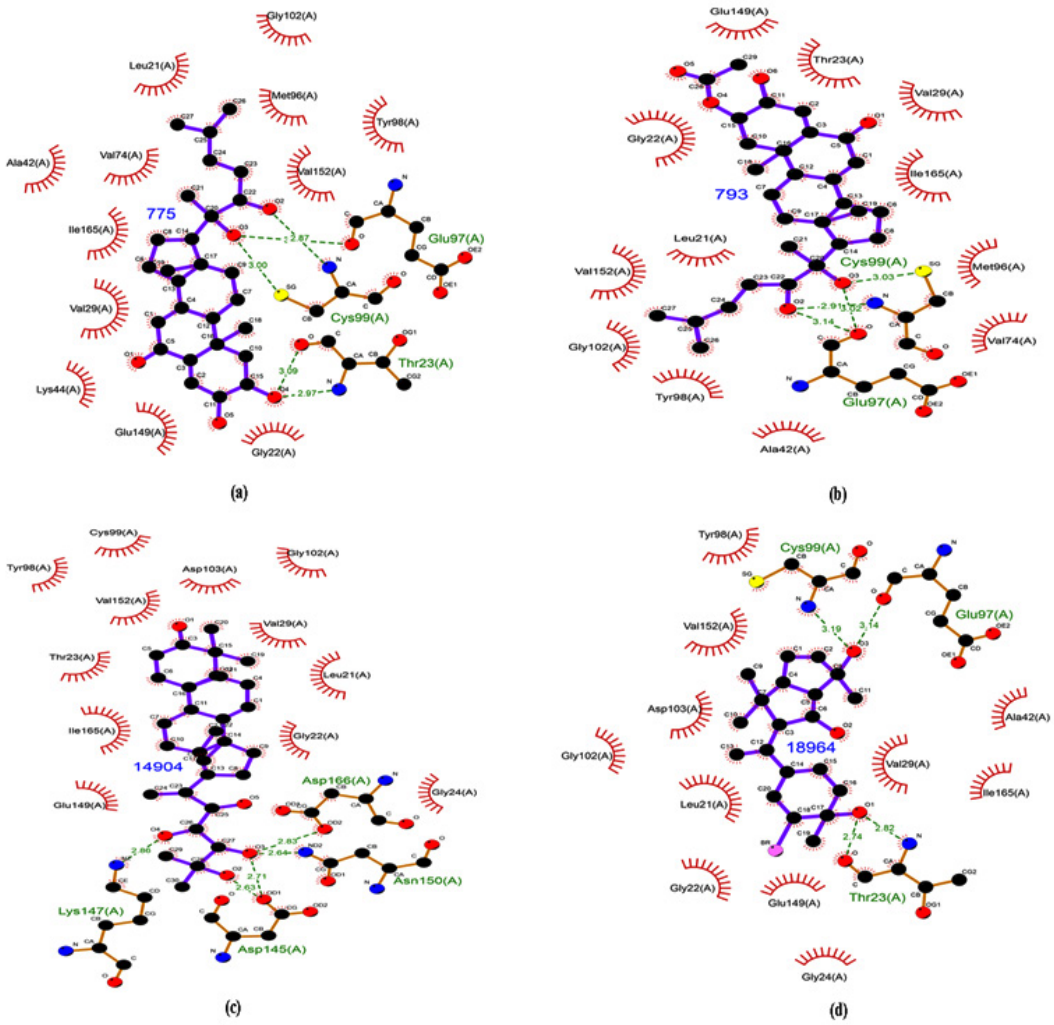

Fig. 5. The docking site images of IêK protein when docked against ligands: CMNPD 775 (a); CMNPD 793 (b); CMNPD 1490 (c); CMNPD 18964(d)

is an automated docking program that efficiently samples ligand poses within the receptor binding site and estimates the free energy of binding[26-27].

The ligand-receptor contacts analysis (Table 3), after docking studies, provided insight into specific molecular interactions underlying their high predicted affinities. The marine phytochemical 8,11-dihydro-1-methoxylaurokamuren-12-ol (CMNPD25050) was observed to be the ligand with highest affinity towards human IêK protein with lowest binding energy of -11.35 kCal/mol (Table 2) and was observed to form hydrogen bonds with key IêK protein residues Cys99, and Asp166 (Table 3), which stabilized the ligand within the active site of receptor protein. The hydroxyl group of ligands was revealed to act as both hydrogen bond donor and acceptor to these critical binding site residues of IêK protein. Additionally, the hydrophobic contacts with Leu21, Gly22, and other non-polar residues can be predicted to improve complementarity and further reinforce binding. These observed intermolecular interactions with similar binding pocket compared to Curcumin (Table 3 and Figure 6) provide clues into the structural basis of 8,11-dihydro-1-methoxylaurokamuren-12-ol's high predicted affinity and warrant the highest priority for subsequent experimental IêK enzyme inhibition assays at *in-vitro* and *in-vivo* level as anti-inflammatory leads with improved potency and pharmacokinetics over current standards like curcumin. Other studied marine phytochemicals (CMNPD793, CMNPD775, CMNPD18964, CMNPD14904, CMNPD31514 and CMNPD24296) have binding affinity better than curcumin (with binding energy of – 8.63 kCal/mol) (Table 2,3 and Figure 5,6) were observed to be produced by the marine genera *Ceriops* and

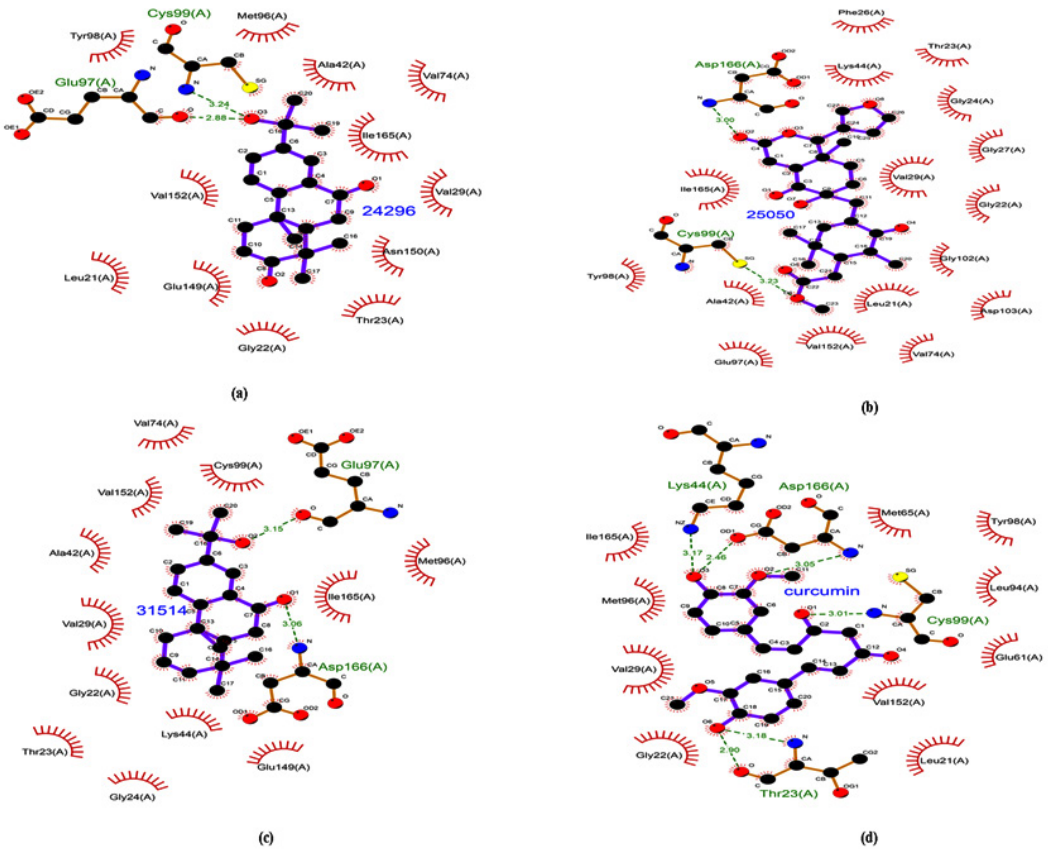

Fig. 6. The docking site images of IêK protein when docked against ligands: CMNPD 24296 (a); CMNPD 25050 (b); CMNPD 31514 (c) and Curcumin (d)

Laurencia (Table 2). The alcoholic extract of *Ceriops decandra* has been identified for its anti-inflammatory properties[43-44], antioxidant activity[45], antidiarrhoeal activity[46] and Hepatoprotective[47]. The crude extracts of *Laurencia obtusa* have been reported for pharmacological activities like *in-vivo* anti-inflammatory, *in-vitro* immunomodulatory, gastroprotective and analgesic effects in earlier reported studies[48-49]. *Laurencia tristicha* and *Laurencia obtusa* have been reported to have antioxidant properties[49-50]. These studies provide evidence that marine algae produce compounds with neuroprotective and anti-inflammatory activities relevant to Alzheimer's disease. While the specific mechanisms were not characterized, the origins of the hit compounds suggest they may exhibit similar therapeutic benefits and target neurotoxic inflammation linked to Alzheimer's progression. The predicted IêK binding and inhibitory activities of the identified phytochemicals are consistent with potential anti-inflammatory effects mediated through modulation of the NF-kB/IêK pathway. Molecular dynamics simulations of the top hit marine phytochemical 8,11-dihydro-1-methoxy laurokamuren-12-ol in complex with IêK protein provided insights into binding dynamics(Figure 7). RMSD analysis confirmed a stable binding mode after initial equilibration(Figure 7a). RMSF revealed a dynamic protein structure with flexible regions crucial for ligand binding and conformational changes(Figure 7b). The radius of gyration indicated a relatively compact and stable system throughout the 10 ns simulation, with minor fluctuations reflecting inherent flexibility(Figure 7c). Interaction energy analysis showed favourable electrostatic interactions counterbalanced by unfavourable steric clashes, a common trade-off in molecular recognition(Figure 7e). Variable hydrogen bonding patterns suggested a highly dynamic binding mode contributing to stability and specificity(Figure 7d). SASA fluctuations reinforced the dynamic nature of the system

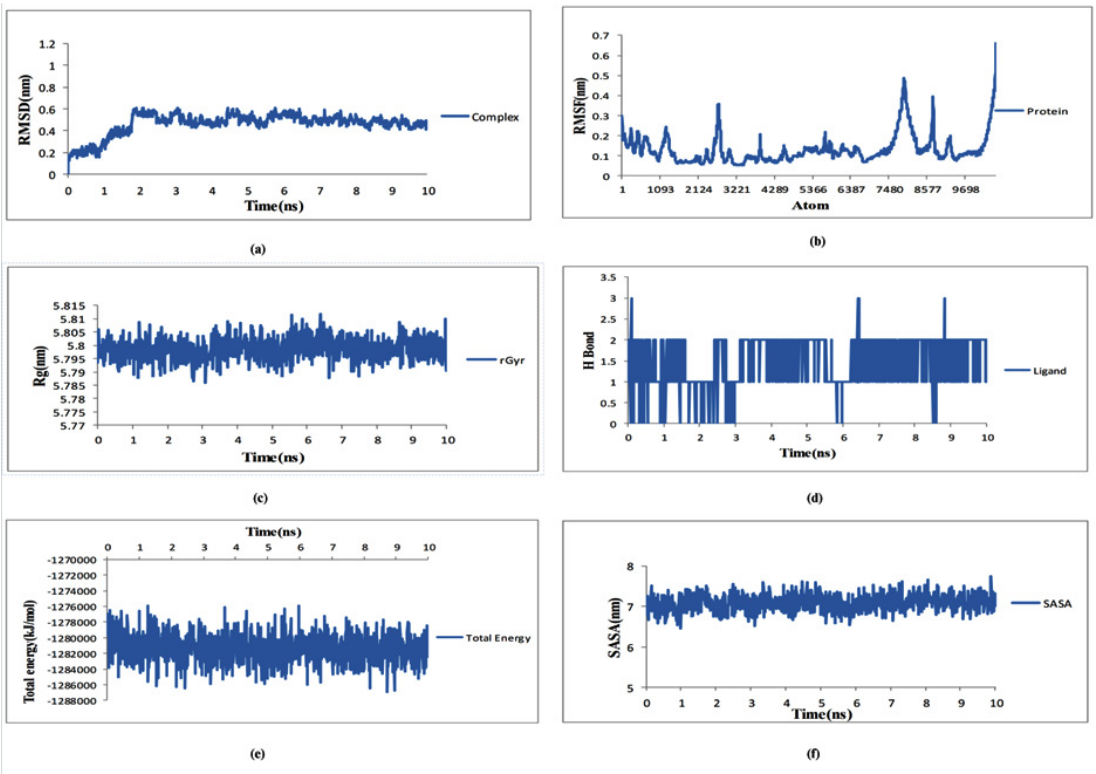

Fig. 7. Molecular dynamic studies of top hit marine phytochemical CMNPD 25050 with IêK protein, RMSD of ligand-protein complex (a); RMSF of protein (b); Total radiation of gyration (c); Hydrogen Bond (d); Total interaction energy (e); SASA (f).

undergoing conformational changes that can modulate biological activity(Figure 7e). Overall, the simulations highlighted the interplay between favourable/unfavourable interactions, dynamic binding mode, and the role of structural flexibility in modulating the phytochemical's bioactivity. Further studies are warranted to confirm the neuroprotective and anti-inflammatory properties of these marine natural product hits.

CONCLUSION

The present *in-silico* study of screening marine phytochemicals for inhibiting human IêK enzyme has provided a good molecular insight into the interactions of human IêK enzyme. The study revealed seven potential inhibitors of the marine phytochemical category as good human IêK enzyme inhibitors and thus potent AD therapeutic options to be evaluated further at *in-vitro* and/or *in-vivo* levels. In particular, 8,11-dihydro-1-methoxylaurokamuren-12-ol with CMNPD ID 25050 is predicted to show maximum inhibition of the human IêK enzyme. The molecular dynamics simulations elucidated the binding dynamics of 8,11-dihydro-1-methoxy laurokamuren-12-ol with NF-êB, revealing the interplay between favourable and unfavorable interactions, and the significance of structural flexibility in modulating bioactivity, thus proposed as most potential AD therapeutics for further evaluations. The virtual high throughput screening study also provides a rational starting point for identifying novel IêK protein-targeted neuroprotective agents from marine sources.

ACKNOWLEDGEMENTS

The authors thank M D University, Rohtak and UGC, New Delhi for providing SJSGC-JRF to AG and M. D. University, Rohtak for providing URS to DS. The authors also thank DBT-BUILDER MDU for providing laboratory facility for the work.

Funding Sources

The author received no financial support for the research, authorship, and/or publication of this article.

Conflict of Interest

The authors do not have any conflicts of interest.

Data Availability Statement

Supplementary data available.

Ethics Approval Statement

The work is original, and it has not been published anywhere.

Authors' Contribution

Both the authors contributed equally.

REFERENCES

1. 2022 Alzheimer's disease facts and figures. *Alzheimers Dement*. 2022;18(4):700-789. doi:10.1002/alz.12638
2. Serrano-Pozo A, Qian J, Muzikansky A, et al. Thal Amyloid Stages Do Not Significantly Impact the Correlation Between Neuropathological Change and Cognition in the Alzheimer Disease Continuum. *J Neuropathol Exp Neurol*. 2016;75(6):516-526. doi:10.1093/jnen/nlw026
3. Jha NK, Jha SK, Kar R, Nand P, Swati K, Goswami VK. Nuclear factor-kappa â as a therapeutic target for Alzheimer's disease. *J Neurochem*. 2019;150(2):113-137. doi:10.1111/jnc.14687
4. Gupta SC, Kim JH, Prasad S, Aggarwal BB. Regulation of survival, proliferation, invasion, angiogenesis, and metastasis of tumor cells through modulation of inflammatory pathways by nutraceuticals. *Cancer Metastasis Rev*. 2010;29(3):405-434. doi:10.1007/s10555-010-9235-2
5. Liu S, Misquitta YR, Olland A, et al. Crystal structure of a human IêB kinase â asymmetric dimer. *J Biol Chem*. 2013;288(31):22758-22767. doi:10.1074/jbc.M113.482596
6. Snow WM, Albensi BC. Neuronal Gene Targets of NF-êB and Their Dysregulation in Alzheimer's Disease. *Front Mol Neurosci*. 2016;9:118. Published 2016 Nov 9. doi:10.3389/fnmol.2016.00118
7. Ahn HJ, Hernandez CM, Levenson JM, Lubin FD, Liou HC, Sweatt JD. c-Rel, an NF-kappaB family transcription factor, is required for hippocampal long-term synaptic plasticity and memory formation. *Learn Mem*. 2008;15(7):539-549. Published 2008 Jul 11. doi:10.1101/lm.866408
8. O'Riordan KJ, Huang IC, Pizzi M, et al. Regulation of nuclear factor kappaB in the hippocampus by group I metabotropic glutamate receptors. *J Neurosci*. 2006;26(18):4870-4879. doi:10.1523/JNEUROSCI.4527-05.2006
9. Chen CH, Zhou W, Liu S, et al. Increased NF-êB signalling up-regulates BACE1 expression and its therapeutic potential in Alzheimer's disease. *Int J Neuropsychopharmacol*. 2012;15(1):77-90.

doi:10.1017/S1461145711000149

10. Grivennikov SI, Greten FR, Karin M. Immunity, inflammation, and cancer. *Cell*. 2010;140(6):883-899. doi:10.1016/j.cell.2010.01.025
11. Miller BS, Zandi E. Complete reconstitution of human IkappaB kinase (IKK) complex in yeast. Assessment of its stoichiometry and the role of IKKgamma on the complex activity in the absence of stimulation. *J Biol Chem*. 2001;276(39):36320-36326. doi:10.1074/jbc.M104051200
12. Nyiew KY, Ngu EL, Wong KH, Goh BH, Yow YY. Neuroprotective potential of marine algal antioxidants. In: Marine Antioxidants. Elsevier; 2023:341-353. Accessed December 22, 2023. https://www.sciencedirect.com/science/article/pii/B9780323950862000308
13. Silva J, Martins A, Alves C, et al. Natural Approaches for Neurological Disorders-The Neuroprotective Potential of *Codium tomentosum*. *Molecules*. 2020;25(22):5478. Published 2020 Nov 23. doi:10.3390/molecules25225478
14. Zhou X, Yi M, Ding L, He S, Yan X. Isolation and Purification of a Neuroprotective Phlorotannin from the Marine Algae *Ecklonia maxima* by Size Exclusion and High-Speed Counter-Current Chromatography. *Mar Drugs*. 2019;17(4):212. Published 2019 Apr 4. doi:10.3390/md17040212
15. Kim TK, Hong JM, Kim KH, et al. Potential of Ramalin and Its Derivatives for the Treatment of Alzheimer's Disease. *Molecules*. 2021;26(21):6445. Published 2021 Oct 26. doi:10.3390/molecules26216445
16. Lyu C, Chen T, Qiang B, et al. CMNPD: a comprehensive marine natural products database towards facilitating drug discovery from the ocean. *Nucleic Acids Res*. 2021;49(D1):D509-D515. doi:10.1093/nar/gkaa763
17. Jayaram B, Singh T, Mukherjee G, Mathur A, Shekhar S, Shekhar V. Sanjeevini: a freely accessible web-server for target-directed lead molecule discovery. *BMC Bioinformatics*. 2012;13 Suppl 17(Suppl 17):S7. doi:10.1186/1471-2105-13-S17-S7
18. Xiong G, Wu Z, Yi J, et al. ADMETlab 2.0: an integrated online platform for accurate and comprehensive predictions of ADMET properties. *Nucleic Acids Res*. 2021;49(W1):W5-W14. doi:10.1093/nar/gkab255
19. Kim S, Chen J, Cheng T, et al. PubChem 2019 update: improved access to chemical data. *Nucleic Acids Res*. 2019;47(D1):D1102-D1109. doi:10.1093/nar/gky1033
20. Forli S, Huey R, Pique ME, Sanner MF, Goodsell DS, Olson AJ. Computational protein-ligand docking and virtual drug screening with the AutoDock suite. *Nat Protoc*. 2016;11(5):905-919. doi:10.1038/nprot.2016.051
21. Pettersen EF, Goddard TD, Huang CC, et al. UCSF Chimera—a visualization system for exploratory research and analysis. *J Comput Chem*. 2004;25(13):1605-1612. doi:10.1002/jcc.20084
22. Burley SK, Bhikadiya C, Bi C, et al. RCSB Protein Data Bank: powerful new tools for exploring 3D structures of biological macromolecules for basic and applied research and education in fundamental biology, biomedicine, biotechnology, bioengineering and energy sciences. *Nucleic Acids Res*. 2021;49(D1):D437-D451. doi:10.1093/nar/gkaa1038.
23. Colovos C, Yeates TO. Verification of protein structures: patterns of nonbonded atomic interactions. *Protein Sci*. 1993;2(9):1511-1519. doi:10.1002/pro.5560020916
24. Laskowski RA, Rullmannn JA, MacArthur MW, Kaptein R, Thornton JM. AQUA and PROCHECK-NMR: programs for checking the quality of protein structures solved by NMR. *J Biomol NMR*. 1996;8(4):477-486. doi:10.1007/BF00228148
25. Wiederstein M, Sippl MJ. ProSA-web: interactive web service for the recognition of errors in three-dimensional structures of proteins. *Nucleic Acids Res*. 2007;35(Web Server issue):W407-W410. doi:10.1093/nar/gkm290
26. Forli S, Huey R, Pique ME, Sanner MF, Goodsell DS, Olson AJ. Computational protein-ligand docking and virtual drug screening with the AutoDock suite. *Nat Protoc*. 2016;11(5):905-919. doi:10.1038/nprot.2016.051
27. Morris GM, Huey R, Lindstrom W, et al. AutoDock4 and AutoDockTools4: Automated docking with selective receptor flexibility. *J Comput Chem*. 2009;30(16):2785-2791. doi:10.1002/jcc.21256
28. Laskowski RA, Swindells MB. LigPlot+: multiple ligand-protein interaction diagrams for drug discovery. *J Chem Inf Model*. 2011;51(10):2778-2786. doi:10.1021/ci200227u
29. Abraham MJ, Murtola T, Schulz R, et al. GROMACS: High performance molecular simulations through multi-level parallelism from laptops to supercomputers. *SoftwareX*. 2015;1-2:19-25. doi:https://doi.org/10.1016/j.softx.2015.06.001
30. Pronk S, Páll S, Schulz R, et al. GROMACS 4.5: a high-throughput and highly parallel open-source molecular simulation toolkit. *Bioinformatics*. 2013;29(7):845-854.

doi:10.1093/bioinformatics/btt055

31. Huang J, Rauscher S, Nawrocki G, et al. CHARMM36m: an improved force field for folded and intrinsically disordered proteins. *Nat Methods*. 2017;14(1):71-73. doi:10.1038/nmeth.4067
32. Veber DF, Johnson SR, Cheng HY, Smith BR, Ward KW, Kopple KD. Molecular properties that influence the oral bioavailability of drug candidates. *J Med Chem*. 2002;45(12):2615-2623. doi:10.1021/jm020017n
33. Wang NN, Huang C, Dong J, et al. Predicting human intestinal absorption with modified random forest approach: a comprehensive evaluation of molecular representation, unbalanced data, and applicability domain issues. *RSC advances*. 2017;7(31):19007-19018.
34. Liu L, Fu L, Zhang JW, et al. Three-Level Hepatotoxicity Prediction System Based on Adverse Hepatic Effects. *Mol Pharm*. 2019;16(1):393-408. doi:10.1021/acs.molpharmaceut.8b01048
35. Lei T, Chen F, Liu H, et al. ADMET Evaluation in Drug Discovery. Part 17: Development of Quantitative and Qualitative Prediction Models for Chemical-Induced Respiratory Toxicity. *Mol Pharm*. 2017;14(7):2407-2421. doi:10.1021/acs.molpharmaceut.7b00317
36. Wang S, Sun H, Liu H, Li D, Li Y, Hou T. ADMET Evaluation in Drug Discovery. 16. Predicting hERG Blockers by Combining Multiple Pharmacophores and Machine Learning Approaches. *Mol Pharm*. 2016;13(8):2855-2866. doi:10.1021/acs.molpharmaceut.6b00471
37. Lei T, Li Y, Song Y, Li D, Sun H, Hou T. ADMET evaluation in drug discovery: 15. Accurate prediction of rat oral acute toxicity using relevance vector machine and consensus modelling. *J Cheminform*. 2016;8:6. Published 2016 Feb 1. doi:10.1186/s13321-016-0117-7
38. Sippl MJ. Recognition of errors in three-dimensional structures of proteins. *Proteins*. 1993;17(4):355-362. doi:10.1002/prot.340170404
39. Dhorajiwala TM, Halder ST, Samant L. Comparative in silico molecular docking analysis of l-threonine-3-dehydrogenase, a protein target against African trypanosomiasis using selected phytochemicals. Journal of Applied Biotechnology Reports. 2019;6(3):101-108.
40. Achutha AS, Pushpa VL, Manoj KB. Comparative molecular docking studies of phytochemicals as Jak2 inhibitors using Autodock and ArgusLab. Materials Today: Proceedings. 2021;41:711-716.
41. Tsai YM, Chien CF, Lin LC, Tsai TH. Curcumin and its nano-formulation: the kinetics of tissue distribution and blood-brain barrier penetration. *Int J Pharm*. 2011;416(1):331-338. doi:10.1016/j.ijpharm.2011.06.030
42. Cheng KK, Yeung CF, Ho SW, Chow SF, Chow AH, Baum L. Highly stabilized curcumin nanoparticles tested in an in vitro blood-brain barrier model and in Alzheimer's disease Tg2576 mice. *AAPS J*. 2013;15(2):324-336. doi:10.1208/s12248-012-9444-4
43. Mahmud I, Shahria N, Yeasmin S, et al. Ethnomedicinal, phytochemical and pharmacological profile of a mangrove plant Ceriops Decandra GriffDin Hou. *J Complement Integr Med*. 2018;16(1):10.1515/jcim-2017-0129. Published 2018 Jun 22. doi:10.1515/jcim-2017-0129
44. Hossain H, Moniruzzaman Sk, Nimmi I, et al. Anti-inflammatory and antioxidant activities of the ethanolic extract of Ceriops decandra (Griff.) Ding Hou bark. Orient Pharm Exp Med. 2011;11(4):215-220. doi:10.1007/s13596-011-0037-z
45. Hossain MH, Hassan MM, Jahan IA, Nimmi I, Islam A. Antidiarrhoeal activity, nitric oxide scavenging and total tannin content from the bark of Ceriops decandra (griff.) Ding hou. Int J Pharm Sci Res. 2012;3:1306-1311.
46. Gnanadesigan M, Ravikumar S, Anand M. Hepatoprotective activity of Ceriops decandra (Griff.) Ding Hou mangrove plant against CCl4 induced liver damage. Journal of Taibah University for Science. 2017;11(3):450-457.
47. Lajili S, Azouaou SA, Turki M, Muller CD, Bouraoui A. Anti-inflammatory, analgesic activities and gastro-protective effects of the phenolic contents of the red alga, Laurencia obtusa. European Journal of Integrative Medicine. 2016;8(3):298-306.
48. Lajili S, Deghrigue M, Bel Haj Amor H, Muller CD, Bouraoui A. In vitro immunomodulatory activity and in vivo anti-inflammatory and analgesic potential with gastroprotective effect of the Mediterranean red alga Laurencia obtusa. *Pharm Biol*. 2016;54(11):2486-2495. doi:10.3109/13880209.2016.1160937
49. Zhang J, Shi LY, Ding LP, Liang H, Tu PF, Zhang QY. Antioxidant terpenoids from the red alga *Laurencia tristicha*. *Nat Prod Res*. 2021;35(23):5048-5054. doi:10.1080/14786419.2020.1774762
50. Lajili S, Ammar HH, Mzoughi Z, et al. Characterization of sulfated polysaccharide from Laurencia obtusa and its apoptotic, gastroprotective and antioxidant activities. *Int J Biol Macromol*. 2019;126:326-336. doi:10.1016/j.ijbiomac.2018.12.089